

Elastic Compton scattering from the deuteron and nucleon polarizabilities

D.L. Hornidge, B.J. Warkentin, R. Igarashi, J.C. Bergstrom, E.L. Hallin, N.R. Kolb, R.E. Pywell, D.M. Skopik,
J.M. Vogt

Saskatchewan Accelerator Laboratory, University of Saskatchewan, Saskatoon, Saskatchewan, Canada, S7N 5C6

G. Feldman

Department of Physics, The George Washington University, Washington, D.C. 20052

(July 12, 2018)

Cross sections for elastic Compton scattering from the deuteron were measured over the laboratory angles $\theta_\gamma = 35^\circ$ – 150° . Tagged photons in the laboratory energy range $E_\gamma = 84$ – 105 MeV were scattered from liquid deuterium and detected in the large-volume Boston University NaI (BUNI) spectrometer. Using the calculations of Levchuk and L'vov, along with the measured differential cross sections, the isospin-averaged nucleon polarizabilities in the deuteron were estimated. A best-fit value of $(\bar{\alpha} - \bar{\beta}) = 2.6 \pm 1.8$ was determined, constrained by dispersion sum rules. This is markedly different from the accepted value for the proton of $(\bar{\alpha} - \bar{\beta})_p = 10.0 \pm 1.5 \pm 0.9$.

13.40.Em, 13.60.Fz, 14.20.Dh, 25.20.Dc

Elastic photon scattering from deuterium can, in principle, yield basic information on the substructure of the deuteron and hence the nucleons themselves. Compton scattering from the proton has been used extensively to determine the polarizabilities of the proton (see Ref. [1] and references contained therein). The electric ($\bar{\alpha}_p$) and magnetic ($\bar{\beta}_p$) polarizabilities constitute the first-order responses of the internal structure of the proton to externally applied electric and magnetic fields.

The current status of the proton polarizabilities has been reported in Ref. [1].

$$(\bar{\alpha} - \bar{\beta})_p = 10.0 \pm 1.5 \pm 0.9, \quad (1)$$

$$(\bar{\alpha} + \bar{\beta})_p = 15.2 \pm 2.6 \pm 0.2, \quad (2)$$

where the first error is the combined statistical and systematic, and the second is due to the model dependence of the dispersion-relation extraction method. The units of $\bar{\alpha}$ and $\bar{\beta}$ are 10^{-4} fm^3 . There is also a dispersion sum rule which relates the sum of the polarizabilities to the nucleon photoabsorption cross section. The generally accepted result for the Baldin sum rule [2] is

$$(\bar{\alpha} + \bar{\beta})_p = 14.2 \pm 0.5, \quad (3)$$

although recent reevaluations yield 13.69 ± 0.14 [3] and $14.0 \pm (0.3 - 0.5)$ [4]. Note that the experimental value (Eq. 2) is in agreement with the sum rule. The polarizabilities, obtained from Eqs. 1 and 3, are

$$\begin{aligned} \bar{\alpha}_p &= 12.1 \pm 0.8 \pm 0.5, \\ \bar{\beta}_p &= 2.1 \mp 0.8 \mp 0.5. \end{aligned} \quad (4)$$

The status of the neutron polarizabilities is much less satisfactory. The majority of measurements of the electric polarizability of the neutron have been done by low-energy neutron scattering from the Coulomb field of a

heavy nucleus. There is considerable disagreement between the two most recent measurements [5,6]. Schmiedmayer *et al.* [5] reported a value for the *static* electric polarizability of $\alpha_n = 12.0 \pm 1.5 \pm 2.0$, where the first uncertainty is statistical and the second systematic. The difference between the static (α) and the Compton ($\bar{\alpha}$) polarizability is small for the neutron. These data have been reinterpreted by Enik *et al.* [7], and they have suggested that a value of $\alpha_n = 7 - 19$ was more appropriate. In a separate experiment, Koester *et al.* [6] have reported a value of $\alpha_n = 0 \pm 5$. Clearly, the current experimental value of α_n has large uncertainties. Once α_n is obtained, β_n can be determined via the sum-rule relation for the neutron [2],

$$(\bar{\alpha} + \bar{\beta})_n = 15.8 \pm 0.5. \quad (5)$$

The recent reevaluations of this sum rule yield 14.40 ± 0.66 [3] and $15.2 \pm (0.3 - 0.5)$ [4].

An alternate method of measuring the neutron polarizabilities is through the use of the quasi-free Compton scattering reaction $d(\gamma, \gamma' n)p$ in which the scattered photon is detected in coincidence with the recoil neutron. In certain kinematic regions, the proton behaves as a spectator and the scattering is primarily from the neutron. There has been one measurement reported on this reaction using bremsstrahlung photons with an endpoint of 130 MeV [8]. However, due to poor statistics, the resulting determination of $\bar{\alpha}_n$ effectively gives only an upper limit. Experiments have recently been completed at Mainz [9], LEGS, and SAL, but results have yet to be reported.

A third method to determine the polarizability of the neutron is through the elastic Compton scattering reaction $d(\gamma, \gamma)d$. The only reported measurement of this reaction was conducted at Illinois [10]. The low photon energy of this experiment resulted in reduced sensitivity

to the polarizabilities and hence large error bars. Since the deuteron amplitude is sensitive to the sum of the proton and neutron polarizabilities, to obtain specific information on the neutron, it is necessary to subtract the proton polarizabilities. More serious concerns are the contributions from meson exchange currents and other nuclear effects. Therefore, the final results for the neutron polarizabilities depend on a model calculation as well as knowledge of the proton polarizabilities.

The present measurement was performed at the Saskatchewan Accelerator Laboratory (SAL). The facility houses a 300 MeV linear accelerator (LINAC) that injects electrons into a pulse-stretcher ring (PSR), producing a nearly continuous wave (CW) electron beam. The LINAC and PSR were used in conjunction with a high-resolution, high-rate photon tagger, a cryogenic target system, and a large-volume NaI detector. Complete details of the experiment can be found in Ref. [11].

The $d(\gamma, \gamma)d$ cross section was measured using tagged photons in the energy range 84–105 MeV with a resolution of 0.3–0.4 MeV. An electron beam of 135 MeV and $\sim 65\%$ duty factor was incident on a $115 \mu\text{m}$ aluminum radiator producing bremsstrahlung photons, which were tagged via the standard photon tagging technique using the SAL photon tagger [12]. The average tagged flux was $\sim 6 \times 10^7$ photons/s integrated over the photon energy range. The tagging efficiency was measured approximately every 8 hours during the experiment by using a lead glass Čerenkov detector directly in the beam to detect photons in coincidence with electrons in the focal plane. The tagging efficiency was approximately 53%.

Photons scattered from the 12.7 cm long, liquid-deuterium target were detected in the large-volume Boston University NaI (BUNI) gamma-ray spectrometer. BUNI is composed of five optically-isolated segments of NaI, each 55.9 cm in length: the core (26.7 cm in diameter) and four quadrants that form an 11.4 cm thick annulus around the core. Since the inelastic contribution to $d(\gamma, \gamma')d$ begins only 2.2 MeV below the elastic peak, it was essential that the photon detector have at least 2% resolution at 100 MeV. The excellent resolution of BUNI is mainly due to the fact that it effectively contains 100% of the electromagnetic showers created by the incident photons. Scattered photons were detected at lab angles of 35° , 60° , 90° , 120° , and 150° .

A zero-degree (or *in-beam*) calibration of the detector was done once, in the middle of the experiment, in order to obtain both the lineshape of BUNI and an energy calibration for the NaI core. The NaI quadrants were calibrated daily with a radioactive source (Th-C).

Figure 1 depicts the BUNI energy spectrum, after randoms have been subtracted, summed over the incident photon energy range. The contribution from empty-target backgrounds has also been subtracted. Each channel in the focal plane of the tagger corresponds to a different incident photon energy and hence a different energy

for the Compton scattered photon. To sum over tagger channels, the detected photon energy in BUNI was shifted to a value corresponding to the maximum incident photon energy of 105 MeV. The magnitude of the shift was determined by which tagger channel registered the photon.

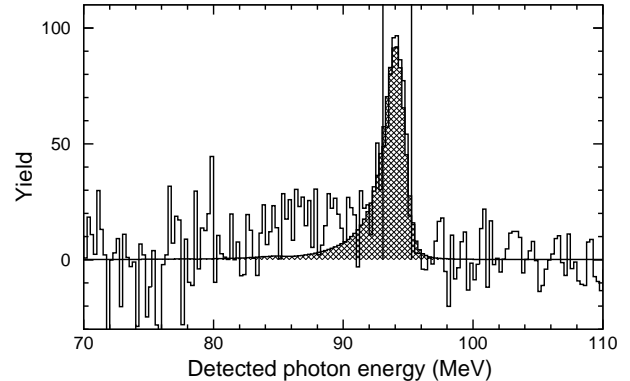


FIG. 1. Photon energy spectrum for $\theta_\gamma = 150^\circ$ showing the lineshape fit (shaded area) to the elastic peak. The inelastic contribution is readily visible. The region of interest is indicated by the vertical lines.

After background subtraction, the elastic peak in the BUNI energy spectrum was integrated over a specific region of interest (ROI), depending on the angle, to obtain the yields. This region was chosen to ensure that no inelastic contributions were contained in the integrated region. The ROI for the 150° photon energy spectrum is shown in Fig. 1 (vertical lines). The inelastic contribution is evident in the energy range 80–90 MeV.

Systematic errors associated with the energy calibration were investigated by comparing the chi-square between the data and the in-beam lineshape for different calibrations. At the 95% confidence level, the uncertainties in the cross sections were 1–4%, depending on angle.

The detection efficiency for the scattered photons was largely constrained by the small size of the ROI and photon absorption before reaching the detector. Since the ROI (Fig. 1) only selected the peak of the elastic scattering distribution, a significant number of events from the tail of the lineshape were excluded. The ROI efficiency was deduced using the zero-degree Compton spectrum, shifted to the appropriate energy, and represents the response of monochromatic photons in BUNI. Comparisons of measurements and EGS simulations of zero degree and scattering geometries [13] confirmed that the lineshape of BUNI measured at zero degrees was consistent with the measured lineshape in the scattering geometry within $\sim 3\%$. The ratio of counts inside the ROI to the total counts in the lineshape yielded an efficiency of $(62 \pm 2)\%$.

The absorption efficiency was broken into two parts:

that due to absorption of photons in the target and associated apparatus, and that due to absorption of photons in the materials located between the NaI crystal and the target enclosure. The first absorption factor was obtained with an EGS simulation [13]. The second was found by integrating the entire zero-degree lineshape from the in-beam calibration and comparing it to the incident photon flux as determined by the photon tagger. The absorption factor was approximately $(89 \pm 1)\%$, which gave an overall detection efficiency of $(55 \pm 2)\%$, relatively independent ($<1\%$) of scattering angle.

The effect of the high-rate photon flux on the measured yield was investigated. Rate effects were found to be $<2\%$ in all cases [11].

Sources of systematic errors in this experiment included target thickness (2.5%), solid angle (1.6%), detection efficiency (3.6%), incident photon flux (1%), and energy calibration (1–4% depending on angle). Adding contributions in quadrature gives a total systematic error of 6.4% (35°), 4.9% (60°), 4.8% (90°), 4.9% (120°), and 5.2% (150°).

The final center-of-mass system (CMS) differential cross sections for the $d(\gamma, \gamma)d$ reaction as a function of CMS scattering angle are displayed in Fig. 2 and are listed in Table I. The data were averaged over the incident photon energy range of 84–105 MeV. The error bars in the figure are the quadratic sum of the statistical and systematic errors.

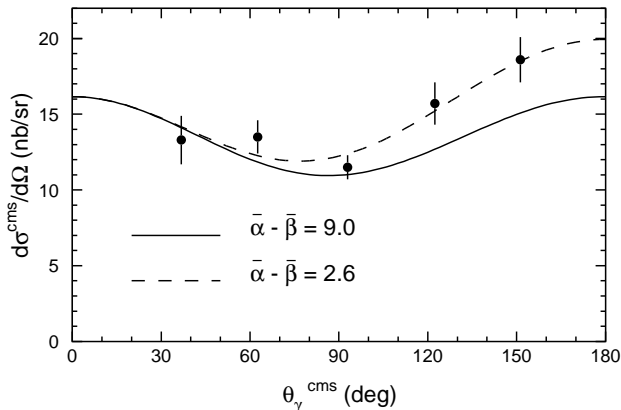


FIG. 2. Differential cross sections for elastic scattering of 84–105 MeV photons from deuterium. The curves are calculations of Levchuk and L’vov with different polarizabilities.

Levchuk and L’vov [4,14] have calculated the differential cross section for the $d(\gamma, \gamma)d$ reaction in the framework of a diagrammatic approach. The scattering amplitude is expressed in terms of resonance and seagull amplitudes. The resonance amplitudes correspond to two-step processes and include rescattering of the intermediate nucleons. The one- and two-body seagull amplitudes involve a photon being absorbed and emitted at

the same moment within the energy scale involved. The one-body seagull diagrams include the nucleon polarizabilities. The contribution of the various ingredients to the $d(\gamma, \gamma)d$ reaction at 94 MeV is illustrated in Fig. 3.

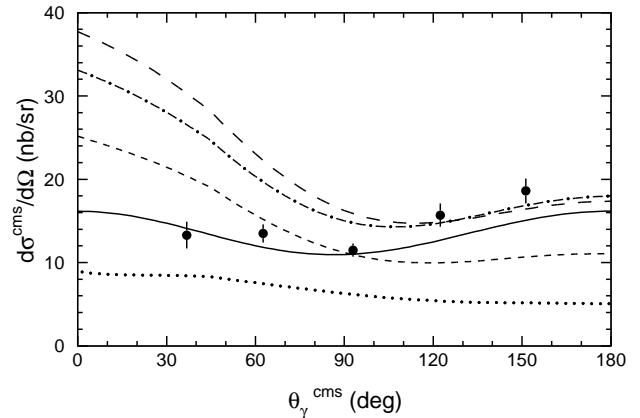


FIG. 3. Theoretical calculations of Levchuk and L’vov for the $d(\gamma, \gamma)d$ differential cross section at $E_\gamma=94$ MeV. The contributions, added successively, are the resonant (dotted), one-body seagull without polarizabilities (short-dashed), two-body seagull (long-dashed), resonant rescattering (dot-dashed), and polarizabilities (solid).

The solid line in Figs. 2 and 3 is the full calculation of Levchuk and L’vov with nominal free values of the isospin-averaged polarizabilities, $\bar{\alpha} = 12.0$, $\bar{\beta} = 3.0$ or $(\bar{\alpha} - \bar{\beta}) = 9.0$. By imposing the sum-rule constraints (Eqs. 3 and 5), the difference of the polarizabilities can be taken as a free parameter and fitted to the experimental data. The dashed curve in Fig. 2 corresponds to the best-fit value of

$$(\bar{\alpha} - \bar{\beta}) = 2.6 \pm 1.8, \quad (6)$$

which was determined by minimizing the chi-square ($\chi^2/N_{d.o.f.} = 2.8/4$) between the calculation and the data. Choosing the sum-rule results of Babusci *et al.* gives a $<4\%$ increase in $(\bar{\alpha} - \bar{\beta})$. The fitted value is substantially different from the nominal free value, and is driven by the back-angle cross sections. The extracted $(\bar{\alpha} - \bar{\beta})$ may be interpreted in terms of (1) medium modifications to the nucleon polarizabilities ($\Delta\bar{\alpha}$ and $\Delta\bar{\beta}$), (2) neutron polarizabilities which are quite different from the proton, or (3) missing physics in the calculation used to extract the polarizabilities. It is important to note that the extracted value of $(\bar{\alpha} - \bar{\beta})$ is dependent upon the theoretical model used. For a discussion of the model dependence of the existing calculations see Refs. [4,14].

Medium modifications to the free polarizabilities for Compton scattering from light nuclei have been postulated [15,16]. Recent measurements on ^4He [17], ^{12}C [13], and ^{16}O [18] have suggested that changes on the order of

$\Delta\bar{\beta} = -\Delta\bar{\alpha} = 4-8$ were required in order to describe the data. These differences were driven by the back-angle cross sections which tended to be larger than the theoretical predictions, as is also seen in the current $d(\gamma, \gamma)d$ results. Other measurements, performed at Lund, have reported no modification of the free polarizabilities [19]. Clearly this issue has yet to be resolved. In the current measurement, modifications of $\Delta\bar{\beta} \sim 3$ would be required to explain the data. However, for a lightly bound system like the deuteron, medium modifications might be expected to be small.

Assuming that the proton polarizabilities are unmodified in the deuteron, the neutron polarizabilities can be extracted from the fitted $(\bar{\alpha} - \bar{\beta})$. Using the fitted value along with Eq. 1 yields

$$(\bar{\alpha} - \bar{\beta})_n = -4.8 \pm 3.9, \quad (7)$$

which can be used along with Eq. 5 to determine the neutron polarizabilities,

$$\begin{aligned} \bar{\alpha}_n &= 5.5 \pm 2.0, \\ \bar{\beta}_n &= 10.3 \mp 2.0. \end{aligned} \quad (8)$$

The error bars do not include any model dependence introduced by the theoretical calculation and are anti-correlated due to application of the sum rule. These results are surprising, since the neutron values are not expected to be radically different from the proton.

Evidence for modification of the backward spin polarizability (γ_π) has been reported [20]. The suggested modification would increase the theoretical back-angle cross sections (Fig. 2) and hence increase the extracted $(\bar{\alpha} - \bar{\beta})$ by ~ 3 . However, a recent measurement of $d(\gamma, \gamma'p)n$ reports no evidence for such a modification of γ_π [21].

There has also been a recent calculation of the $d(\gamma, \gamma)d$ differential cross section within the framework of baryon chiral perturbation theory [22]. The results of the calculation of Beane *et al.*, which includes $O(Q^3)$ terms and only a partial set of the $O(Q^4)$ corrections, are similar in magnitude to that of Levchuk and L'vov. However, Beane *et al.* warn that their prediction at 95 MeV has considerable uncertainty due to the slow convergence of the series. Understanding what physics may be missing in the theoretical calculations will have to wait for the full $O(Q^4)$ treatment.

TABLE I. Center-of-mass differential cross sections for the elastic scattering of 84–105 MeV photons from deuterium. The first error is statistical and the second is systematic.

θ_γ^{lab} (deg)	θ_γ^{cms} (deg)	$d\sigma^{cms}/d\Omega_\gamma$ (nb/sr)
35.0	36.8	$13.3 \pm 1.3 \pm 0.9$
60.0	62.7	$13.5 \pm 0.8 \pm 0.7$
90.0	93.0	$11.5 \pm 0.6 \pm 0.6$
120.0	122.6	$15.7 \pm 1.1 \pm 0.8$
150.0	151.5	$18.6 \pm 1.1 \pm 1.0$

Other theoretical calculations for the $d(\gamma, \gamma)d$ reaction have been reported. The calculations of Karakowski and Miller [23] underpredict the present measurement by a factor of ~ 2 at backward angles when using the nominal free values of the polarizabilities. Wilbois *et al.* [24] have reported a calculation at 100 MeV but with polarizabilities set to zero. Finally, Chen *et al.* [25] have reported results only up to a photon energy of 69 MeV.

Forthcoming results on the quasi-free Compton scattering from the deuteron, with detection of the recoiling nucleon, should shed some light on this controversy. By doing the experiments in quasi-free kinematics (in the energy region $E_\gamma=200-300$ MeV and backward angles for the scattered photons) the model dependence is minimized, and the polarizabilities can be extracted separately for the proton and the neutron.

The authors would like to thank M.I. Levchuk and A.I. L'vov for supplying the code for their theoretical calculations.

This work was supported in part by a grant from the Natural Science and Engineering Research Council of Canada.

-
- [1] B.E. MacGibbon *et al.*, Phys. Rev. C **52**, 2097 (1995).
 - [2] V.A. Petrun'kin, Sov. J. Part. Nucl. **11**, 278 (1981).
 - [3] D. Babusci, G. Giordano, and G. Matone, Phys. Rev. C **57**, 291 (1998).
 - [4] M.I. Levchuk and A.I. L'vov, Nucl. Phys. **A** (submitted); LANL preprint number nucl-th/9909066.
 - [5] J. Schmiedmayer, P. Reihls, J.A. Harvey, and N.W. Hill, Phys. Rev. Lett. **66**, 1015 (1991).
 - [6] L. Koester *et al.*, Phys. Rev. C **51**, 3363 (1995).
 - [7] T.L. Enik, L.V. Mitsyna, V.G. Nikolenko, A.B. Popov, and G.S. Samosvat, Sov. J. Nucl. Phys. **60**, 567 (1997).
 - [8] K.W. Rose *et al.*, Nucl. Phys. **A514**, 621 (1990).
 - [9] F. Wissmann, private communication.
 - [10] M.A. Lucas, Ph.D. Thesis, University of Illinois, 1994.
 - [11] D.L. Hornidge, Ph.D. Thesis, University of Saskatchewan, 1999.
 - [12] J.M. Vogt *et al.*, Nucl. Instrum. Methods Phys. Res. Sect. A **324**, 198 (1993).
 - [13] B.J. Warkentin, M.Sc. Thesis, University of Saskatchewan, 1999.
 - [14] M.I. Levchuk and A.I. L'vov, in Proceedings of the Conference on Mesons and Light Nuclei, Prague-Pruhonice, 1998.
 - [15] M. Ericson and M. Rosa-Clot, Phys. Lett. B **188**, 11 (1987).
 - [16] G.G. Bunatyan, Sov. J. Nucl. Phys. **55**, 1781 (1992).
 - [17] K. Fuhrberg *et al.*, Nucl. Phys. **A591**, 1 (1995).
 - [18] G. Feldman *et al.*, Phys. Rev. C **54**, R2124 (1996).
 - [19] S. Proff *et al.*, Nucl. Phys. **A646**, 67 (1999).
 - [20] J. Tonnison, A.M. Sandorfi, S. Hoblit, A.M. Nathan, Phys. Rev. Lett. **80**, 4382 (1998).

- [21] F. Wissmann *et al.*, Nucl. Phys. **A** (in press).
- [22] S.R. Beane *et al.*, Nucl. Phys. **A** (to be published); LANL preprint number nucl-th/9905023.
- [23] J.J. Karakowski and A. Miller, Phys. Rev. C **60**, 014001 (1999).
- [24] T. Wilbois, P. Wilhelm, and H. Arenhövel, Few-Body Sys. Supp. **9**, 263 (1995).
- [25] J.-W. Chen, H.W. Gießhammer, M.J. Savage, and R.P. Springer, Nucl. Phys. **A644**, 245 (1998).